Progress In Electromagnetics Research M, Vol. 118, 47–57, 2023

Time Domain Coupling Analysis of the Transmission Line Excited by the Leakage EM Fields from the Integrated Circuit with Shielded Enclosure

Zhihong Ye[1, 2, *], Sihao Wang[1], Changchang Lu[1], and Yu Zhang[1]

Abstract—At present, numerical methods suitable for the electromagnetic interference (EMI) analysis of the transmission line (TL) excited by the leakage electromagnetic (EM) fields generated by the integrated circuit (IC) of the electronic device are still rare. An efficient time domain hybrid method, consisting of the dynamic differential evolution (DDE) algorithm, transmission line equations, finite difference time domain (FDTD) method, and nonuniform grid technique, is presented to realize the fast simulation of leakage EM fields to the TL. Firstly, a source reconstruction method based on the DDE algorithm is employed to extract the equivalent dipole array to represent the leakage EM radiation from the IC of the device. Then, the coupling model of the TL excited by the leakage EM fields is constructed by the TL equations and nonuniform grid technique, and solved by the FDTD method to realize the synchronous calculation of the leakage EM field radiation and the transient responses on the TL. Finally, the correctness of the source reconstruction method has been tested, and the accuracy and efficiency of the proposed method have been verified via two simulation cases of the transmission line excited by leakage EM fields arising from IC in free space and shielded enclosure by comparing with that of the MOM method.

1. INTRODUCTION

With the rapid development of wireless communication technology, the working frequencies of the ICs of the electronic devices become higher and higher. It will cause that the electromagnetic energies inevitably radiated from some electronic components of the IC [1, 2] must propagate to the outer space of the device, which are called as leakage electromagnetic fields. Interference signals may be generated on the transmission line close to the device by the radiation of the leakage EM fields of the device, which will propagate into the terminal circuits of the TL to affect the normal operation of the device. Therefore, studying the coupling problem of the transmission line excited by the leakage EM fields from the integrated circuit with shielded enclosure can provide support to improve the electromagnetic safety of the devices.

Because the IC contains many fine electronic components and microstrip traces, it is difficult to construct the whole physical structure of the IC with shielded enclosure and simulate the leakage EM fields generated from the IC via some full-wave algorithms, such as FDTD method [3], method of moments (MOM) [4], and finite element method (FEM) [5].

To avoid directly modeling the fine structure of the IC, equivalent dipole method has been proposed [6–9]. However, this method requires that the IC must be located in the free space, because it needs to use the Green's function to construct the relationship matrix between the dipoles' magnetic

Received 5 April 2023, Accepted 14 June 2023, Scheduled 25 July 2023
* Corresponding author: Zhihong Ye (yezh@cqupt.edu.cn).
[1] School of Communication and Information Engineering, Chongqing University of Posts and Telecommunications, Chongqing 400065, China. [2] Chongqing Institute of Digital Arena, Chongqing 400065, China.

moments and the near magnetic fields of the IC. Under the circumstance, some fast prediction methods based on machine learning for the electromagnetic radiation of the ICs are proposed [10–12]. In these methods, neural network is applied to train the mapping matrix between the equivalent dipoles' locations and the electromagnetic fields on the scanning planes to establish the prediction models. However, these methods can only predict the far magnetic fields of free space, and they cannot obtain the amplitudes and phases of the dipoles.

Furthermore, some source reconstruction methods based on the differential evolution (DE) algorithm have been studied [13, 14]. NP populations (dipole arrays) are needed by these methods, and each population has n dipoles. When the dipole number n is large, the efficiencies of these methods are deeply decreased. Hence, Song et al. proposed a dynamic DE (DDE) algorithm to improve the efficiency of the source reconstruction method [15]. Since only one population with n dipoles is used by the DDE algorithm, the convergence speed of this algorithm is fast. In this article, the source reconstruction method is studied on the basis of the DDE algorithm.

Leakage EM fields generated by the IC will propagate in the outer space of the device and act on the TL to induce interference signals. To avoid meshing the fine structure of the TL directly, some efficient field-line hybrid methods have been proposed, such as Baum-Liu-Tesche (BLT) equation [16, 17], FDTD-SPICE method [18], and FDTD-TL method [19–22]. The traditional BLT equation, based on the electromagnetic topology theory, is to construct the relationship matrix between the leakage EM fields and responses on the nodes of the TL. However, it is a frequency domain method and can only obtain the responses on the terminal loads of the TL. FDTD-SPICE and FDTD-TL are both time-domain algorithms and widely applied to the time domain coupling analysis of the TL excited by ambient wave. However, FDTD-SPICE requires tedious theoretical derivation when establishing the SPICE equivalent circuit model of the TL, and the leakage EM field radiation and the transient responses on the TL are calculated respectively. Compared with FDTD-SPICE, the significant feature of FDTD-TL method is that it can achieve the synchronous computation of leakage EM fields and transient responses on the TL.

Therefore, an efficient time domain hybrid method, consisting of the source reconstruction method based on the DDE algorithm and FDTD-TL method, is presented to achieve the fast coupling simulation of the TL excited by the leakage EM fields arising from the IC to avoid the direct mesh division of the fine structures of the IC with device enclosure and the TL. The detailed implementation process of this proposed method will be introduced as follows.

2. THEORY OF THE HYBRID METHOD

The coupling model of the transmission line excited by the leakage electromagnetic fields of the integrated circuit with shielded enclosure is shown in Fig. 1. The leakage EM fields generated by the IC will propagate in the inner space of the device and couple to the outer space via the slots or holes on the shielded enclosure of the IC. Then, the leakage EM fields acting on the TL should couple

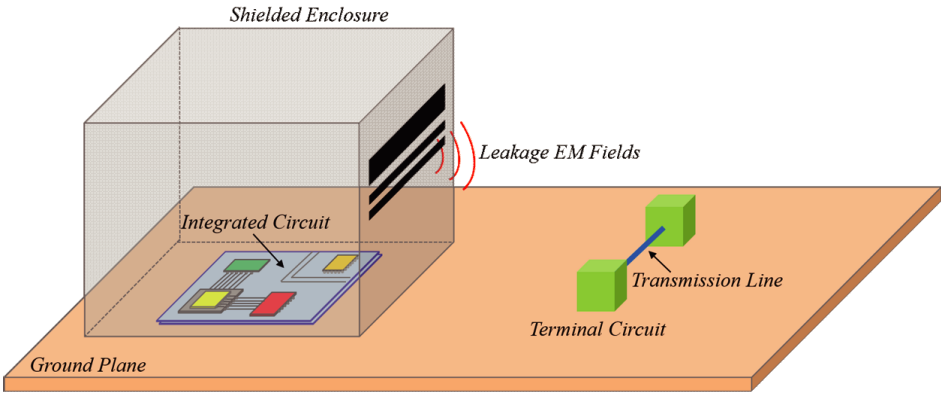

Figure 1. Coupling model of the TL excited by leakage EM fields.

interference signals to disturb the normal operation of the terminal circuits.

The proposed time domain hybrid method applied to the coupling analysis of the TL excited by the leakage EM fields includes three steps.

Firstly, the equivalent dipole array representing the original radiation of the IC in electronic device is constructed via the DDE algorithm with the image theorem and antenna radiation theory.

Secondly, the FDTD method combining with the nonuniform grid technique is employed to compute the radiation electromagnetic fields of the equivalent dipole array.

Finally, the TL equations are utilized to build the coupling model of the TL excited by the leakage EM fields and solved by the FDTD to obtain the transient responses on the TL rapidly.

Next, the implementation process of this proposed hybrid method will be introduced in detail from three aspects of the equivalent source modeling of the leakage EM fields, FDTD calculation for the radiation fields generated by the equivalent dipole array and coupling analysis of the leakage EM fields acting on the TL.

2.1. Source Reconstruction Modeling of the Leakage EM Fields

In this section, the implementation process of the source reconstruction method based on the DDE algorithm employed to reconstruct the equivalent source of the IC with device enclosure on the ground plane will be introduced.

Firstly, an equivalent magnetic dipole array that can generate the same EM fields above the ground as the unknown IC structure based on the equivalence principle is placed on a two-dimensional plane parallel to the slots and/or holes, as shown in Fig. 2. Here, the normal directions of the slots and/or holes are assumed as the x-direction, and the magnetic moments of each dipole of the dipole array contain two components M_y and M_z.

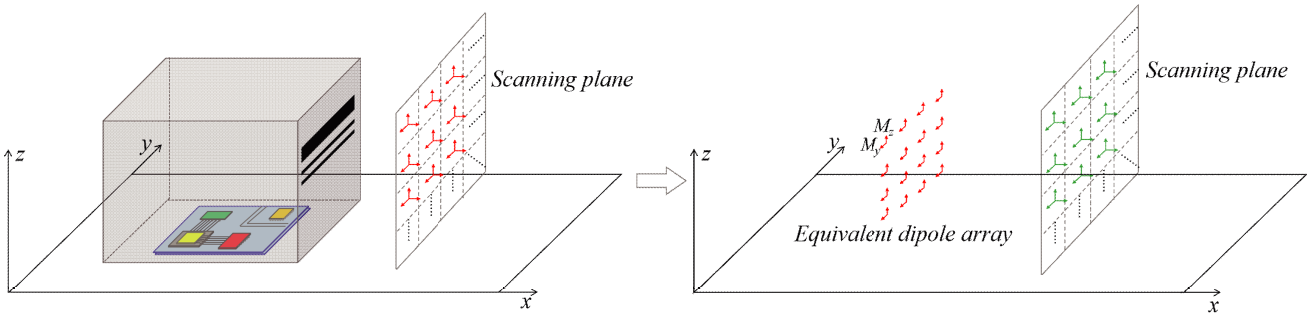

Figure 2. Equivalent dipole array model of the IC with device enclosure.

In this article, the near magnetic fields of the IC with shielded enclosure on the scanning plane are extracted by the MOM method instead of the near-field scanning technique [23] normally used due to the constraint of our team's experimental condition. Therefore, the known structure of an IC with shielded enclosure is constructed when verifying the correctness of the source reconstruction method later.

Then the DDE algorithm is employed to obtain the magnetic moments of the equivalent dipole array. Here, only one population is used in the DDE, which contains NP dipoles, where NP is the dipole number. The individuals of the population are the magnetic moments of these dipoles, which can be expressed as

$$\mathbf{X}_i = \{\mathrm{Re}\left(M_{y,i}\right), \mathrm{Im}\left(M_{y,i}\right), \mathrm{Re}\left(M_{z,i}\right), \mathrm{Im}\left(M_{z,i}\right)\} \tag{1}$$

where $\mathbf{X}_i$ represents the moment vector of the i-th dipole. $M_{y,i}$ and $M_{z,i}$ are the dipole moments along y and z directions of the i-th dipole respectively. Re and Im represent the real and imaginary components of the dipole moments.

In DDE, every dipole should be initialized and dynamically updated by mutation, crossover, and selection process.

1) Initialization: the dipole's magnetic moments of these individuals are randomly initialized as

$$\mathbf{X}_i^{\text{initial}} = \mathbf{A}^L + \text{rand} \times \left(\mathbf{A}^U - \mathbf{A}^L\right) \tag{2}$$

where $\mathbf{X}_i^{\text{initial}}$ represents the initialized moment vector of the i-th dipole. $\mathbf{A}^U$ and $\mathbf{A}^L$ are the upper and lower value ranges of the moment vectors of all dipoles. rand is a random number in the range [0, 1].

2) Mutation: the i-th parent dipole is mutated via the "DE/rand/1" strategy [24], which is expressed as

$$\mathbf{V}_i^g = \mathbf{X}_{r1}^g + F\left(\mathbf{X}_{r2}^g - \mathbf{X}_{r3}^g\right) \tag{3}$$

where g stands for the current iteration. $\mathbf{V}_i^g$ is the moment vector of the i-th mutant dipole. $\mathbf{X}_{r1}^g$, $\mathbf{X}_{r2}^g$, and $\mathbf{X}_{r3}^g$ are the moment vectors of three parent dipoles, where r_1, r_2, and r_3 are three randomly selected integers from the range [1, NP]. F is the scaling factor.

3) Crossover: The four elements of the i-th children dipole are formed by

$$U_{i,j}^g = \begin{cases} V_{i,j}^g, & \text{rand} \le \text{CR} \\ x_{i,j}^g, & \text{otherwise} \end{cases}, \quad i = 1, ..., \text{NP}, \;\; j = 1, ..., 4 \tag{4}$$

where CR is the predefined crossover factor.

4) Selection: the near magnetic fields generated by the moment vectors of the i-th children dipole $\mathbf{U}_i^g$ and i-th parent dipole $\mathbf{X}_i^g$ with other dipoles' moment vectors are compared with that of reference magnetic fields of the original model of IC to determine the new i-th individual, which is expressed as

$$\mathbf{X}_i^{g+1} = \begin{cases} \mathbf{U}_i^g, & \delta_i^g \le \delta_p^g \\ \mathbf{X}_i^g, & \text{otherwise} \end{cases}, \quad i = 1, ..., \text{NP} \tag{5}$$

where

$$\delta_p^g = \sqrt{\frac{\sum_{m=1}^{M} \left(\left| H\left(\mathbf{X}_1^g, ..., \mathbf{X}_{\text{NP}}^g\right)\right|_m - \left|H^{ref}\right|_m \right)^2}{\sum_{m=1}^{M} \left(\left|H^{ref}\right|_m \right)^2}} \tag{6}$$

$$\delta_i^g = \sqrt{\frac{\sum_{m=1}^{M} \left(\left| H\left(\mathbf{Y}_1^g, ..., \mathbf{Y}_{i-1}^g, \mathbf{U}_i^g, \mathbf{Y}_{i+1}^g, ..., \mathbf{Y}_{\text{NP}}^g\right)\right|_m - \left|H^{ref}\right|_m \right)^2}{\sum_{m=1}^{M} \left(\left|H^{ref}\right|_m \right)^2}} \tag{7}$$

where M is the observation point number of scanning magnetic fields. δ_p^g and δ_i^g represent the cost functions of all parent dipoles and all children dipoles at the g-th iteration, respectively. $\left|H(\mathbf{X}_1^g, ..., \mathbf{X}_{\text{NP}}^g)\right|$ and $\left|H(\mathbf{Y}_1^g, ..., \mathbf{Y}_{i-1}^g, \mathbf{U}_i^g, \mathbf{Y}_{i+1}^g, ..., \mathbf{Y}_{\text{NP}}^g)\right|$ stand for the scanning magnetic fields generated by the magnetic moments of all parent dipoles and all children dipoles, respectively. These magnetic fields are computed by the superposition of the radiation fields of the equivalent dipole array and its mirror dipole array, and the corresponding calculation formulas can be found from [15]. $|H^{ref}|$ stands for the reference magnetic fields from the original model of IC by the MOM simulation.

The above iteration process is repeated until all dipoles of the population are updated. When the maximum iteration number is reached, or the cost function is small enough, the optimization of the DDE is finished. Then, the equivalent dipole array model of the IC with shielded enclosure is obtained.

2.2. FDTD Calculation for the Radiation Fields of the Dipole Array

Calculating the radiation fields of the dipole array having high precision is the foundation for the further coupling analysis of the transmission line. To avoid meshing the entire computation region in excessively

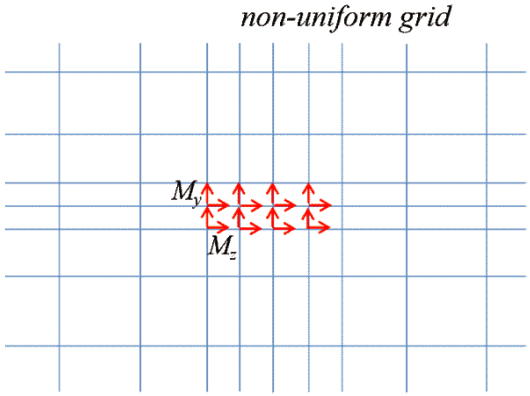

Figure 3. Non-uniform grid division of the computation region.

fine grid depending on the dipole distance of the dipole array, nonuniform grid technique is employed. It means that fine grid is used to mesh the dipole array region, and other regions are meshed via coarse grid, as shown in Fig. 3.

According to the relationship between the magnetic current $\mathbf{J}_m$ and magnetic moment $\mathbf{M}$, the electromagnetic radiation generated by a magnetic dipole can be described by the Maxwell's equation as

$$\nabla \times \mathbf{E} = -\mu \frac{\partial \mathbf{H}}{\partial t} - \mathbf{J}_m = -\mu_0 \frac{\partial \mathbf{H}}{\partial t} - \frac{\mu_0}{\Delta x \Delta y \Delta z} \frac{\partial \mathbf{M}}{\partial t} \tag{8}$$

where $\mathbf{E}$ and $\mathbf{H}$ are the electric field vector and magnetic field vector, respectively. μ_0 is the permeability of free space. Δx, Δy, and Δz are the space steps of the FDTD used in the x, y, and z directions, respectively, which are gradually changed due to the usage of nonuniform grids.

Here, taking the magnetic moment M_y of one dipole as an example to explain the FDTD iteration solutions for the radiation fields of the dipole array. Under the circumstance, Equation (8) is transformed to a scalar equation and written as

$$\frac{\partial E_x}{\partial z} - \frac{\partial E_z}{\partial x} = -\mu_0 \frac{\partial H_y}{\partial t} - \frac{\mu_0}{\Delta x \Delta y \Delta z} \frac{\partial M_y}{\partial t} \tag{9}$$

Because of the M_y formed by amplitude and phase, it can be represented by the trigonometric function in time domain as $M_0 \cos(\omega_0 t + \varphi_m)$, where M_0 and φ_m are the amplitude and phase of M_y, and ω_0 is the angular frequency.

Substituting the time domain expression of the M_y into Equation (9), it can be written as

$$\frac{\partial H_y}{\partial t} = \frac{1}{\mu_0} \left(\frac{\partial E_z}{\partial x} - \frac{\partial E_x}{\partial z} \right) + \frac{M_0 \omega_0 \sin(\omega_0 t + \varphi_m)}{\Delta x \Delta y \Delta z} \tag{10}$$

Using the difference scheme of FDTD to discretize Equation (10) to get the FDTD iteration formula of H_y at the location of M_y is expressed as

$$\begin{aligned} & H_y^{n+\frac{1}{2}} \left(i + \frac{1}{2}, j, k + \frac{1}{2} \right) \\ = \; & H_y^{n-\frac{1}{2}} \left(i + \frac{1}{2}, j, k + \frac{1}{2} \right) \\ & + \frac{\Delta t}{\mu_0} \left[\frac{E_z^n \left(i+1, j, k+\frac{1}{2} \right) - E_z^n \left(i, j, k+\frac{1}{2} \right)}{\Delta x} - \frac{E_x^n \left(i+\frac{1}{2}, j, k+1 \right) - E_x^n \left(i+\frac{1}{2}, j, k \right)}{\Delta z} \right] \\ & + \frac{\Delta t M_0 \omega_0}{\Delta x \Delta y \Delta z} \sin \left(\omega_0 n \Delta t + \varphi_m \right) \end{aligned} \tag{11}$$

The FDTD iteration formulas of other magnetic fields at the locations of the magnetic moments can also be derived as the M_y.

2.3. Coupling Analysis of Leakage EM Fields to the TL

Generally, the distance between the TL and conductive board is often smaller than the minimum wavelength of the leakage fields, so the radiation effect of the TL can be negligible. Under the circumstance, the coupling model of the TL radiated by the leakage fields can be accurately described by the time domain TL equations as

$$\frac{\partial}{\partial y} V(y,t) + L\frac{\partial}{\partial t} I(y,t) = V_F(y,t) \tag{12}$$

$$\frac{\partial}{\partial y} I(y,t) + C\frac{\partial}{\partial t} V(y,t) = I_F(y,t) \tag{13}$$

where $V(y,t)$ and $I(y,t)$ represent the voltage and current vectors on the TL. L and C are the per unit length inductance and capacitance of the TL, respectively, which can be calculated via the empirical formulas found from [25]. $V_F(y,t)$ and $I_F(y,t)$ are the distribution voltage and current source terms of the TL equations, which are determined by the radiation fields of the equivalent dipole array surrounding the TL in absence of the fine TL structure. The specific calculation formulas of the distribution source terms can be found from [22]. Here, the radiation fields of the dipole array are computed via the FDTD method presented in Section 2.2.

Then, the FDTD's central difference scheme is utilized to discretize the TL equations to obtain the transient voltage and current responses on the TL and its terminal loads. The specific iteration formulas of the voltages and currents can be obtained from [19].

3. NUMERICAL SIMULATION

In this section, the correctness of the source reconstruction method is verified firstly. Then, two cases about the coupling of the TL excited by leakage EM fields in the open space and shielded enclosure are simulated by the proposed hybrid method and MOM to verify the accuracy and efficiency of this method.

3.1. Correctness Verification of the Source Reconstruction Method

The known structure of the IC with shielded enclosure is shown in Fig. 4, where the dimensions of the ground plane and shielded enclosure are $L_s \times W_s \times H_s = 40\,\text{cm} \times 60\,\text{cm} \times 1\,\text{cm}$ and $L_c \times W_c \times H_c = 5\,\text{cm} \times 8\,\text{cm} \times 8\,\text{cm}$, respectively, and the size of the rectangular hole on the right surface of the enclosure is $2\,\text{cm} \times 2\,\text{cm}$. The thickness of the enclosure is 1 cm. The IC is located on the central plane of the enclosure, and its size is $6\,\text{cm} \times 7\,\text{cm} \times 0.1\,\text{cm}$. The material of the substrate is FR4 with relative

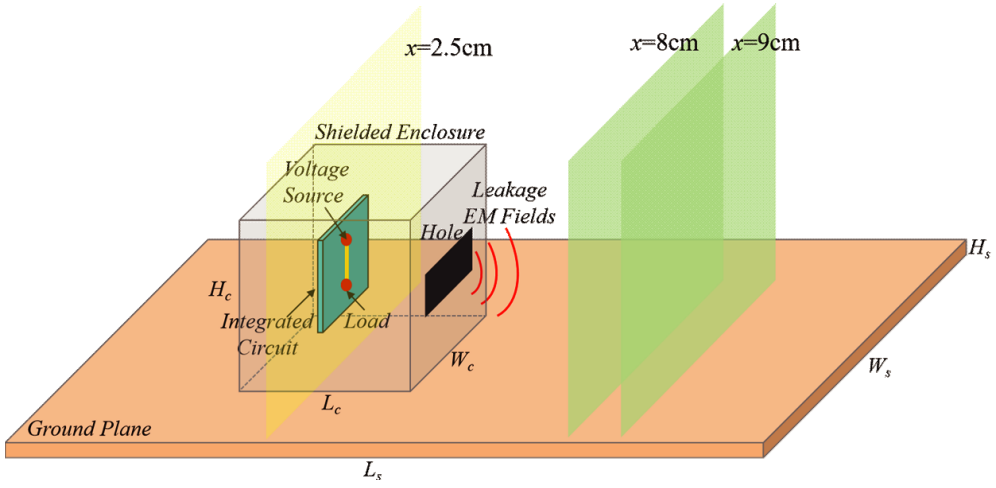

Figure 4. Known structure of the IC with shielded enclosure.

permittivity 4.3 and tangent loss 0.02. The microstrip trace with length 40 mm and width 4 mm is located on the surface of the substrate. A lumped voltage source with amplitude 1 V and frequency 1 GHz is connected to the beginning port of the trace, and the ending port of the trace is a load with the resistance of 50 Ω.

The near magnetic fields on the scanning plane ($x = 8$ cm) with distance 3 cm away from the right surface of the shielding enclosure to the scanning plane are extracted by the MOM as reference, where the size of the scanning plane is 12 cm × 9 cm with a 3 mm sampling interval.

Then, the source reconstruction method based on the DDE is employed to construct the equivalent dipole array of the IC model based on the reference magnetic fields. In our DDE, the dipole array (population) contains 81 dipoles and is located on the plane with $x = 2.5$ cm, which has the size of 4 cm × 4 cm. The dipoles' position is fixed, which can reduce the number of optimization parameters and improve the optimization efficiency. Meanwhile, the crossover parameter CR and scaling factor F are both set as 0.5.

To verify the correctness of the source reconstruction method, the comparison of the magnetic fields $|H_y|$ and $|H_z|$ on the plane with $x = 9$ cm obtained by the prediction of the dipole array and the MOM simulation of the original model of IC is given in Fig. 5, and the root mean square errors (RMSEs) of these magnetic fields are calculated, as shown in Table 1, where the RMSE is defined as

$$\mathrm{RMSE} = \sqrt{\frac{\left\| |H|^{\mathrm{cal}} - |H|^{\mathrm{real}} \right\|}{|H|^{\mathrm{real}}}} \tag{14}$$

where $\|\cdot\|$ stands for the Euclidean norm. $|H|^{\mathrm{cal}}$ and $|H|^{\mathrm{real}}$ are the summation of the magnetic fields on the scanning plane obtained by the dipole array and the real IC model, respectively.

It is obvious that the predicted magnetic fields have high precision compared with the reference magnetic fields.

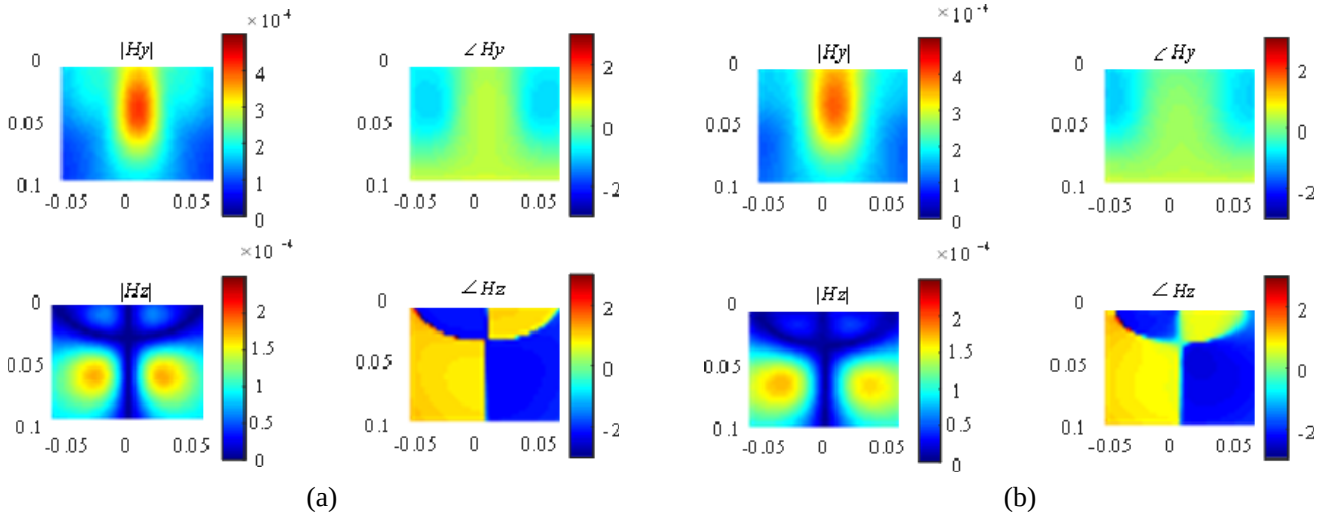

Figure 5. Magnetic fields $|H_y|$ and $|H_z|$ of the two models at the plane with $x = 9$ cm: (a) the magnetic fields of original model, (b) the magnetic fields of equivalent dipole array.

Table 1. RMSE of the magnetic fields obtained by the two models.

Scanning Plane	RMSE of $\lvert H_y \rvert$	RMSE of $\lvert H_z \rvert$
$x = 90$ mm	3.86%	1.64%

3.2. Coupling Simulation of the TL Excited by Leakage EM Fields

The coupling model of the TL on the PEC ground excited by the leakage EM fields arising from the IC is shown in Fig. 6, where the structures of the IC with shielded enclosure and the ground plane are the same as the model used in Section 3.1. The direction of the TL is parallel to the rectangular hole, and the length, height, and radius of the TL are 100 mm, 20 mm, and 1 mm, respectively. The distance of the TL to the shielded enclosure is 4 cm, and the terminal loads of the TL are $R_1 = 50\,\Omega$ and $R_2 = 100\,\Omega$. The maximum and minimum mesh sizes used by the proposed method are 1 cm and 3 mm, respectively.

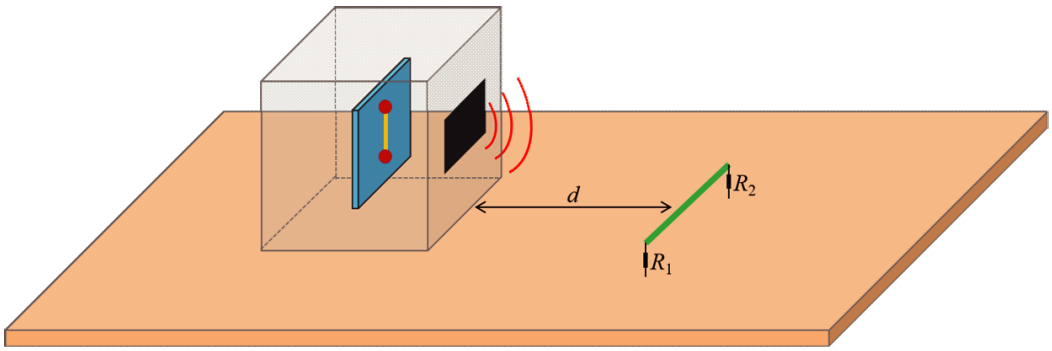

Figure 6. Coupling model of the TL excited by the leakage EM fields.

Figure 7 shows the transient voltages on the terminal loads of the TL computed by the proposed hybrid method and the MOM, where the time domain results of MOM are obtained via the inverse Fourier transform. It should be noted that the whole model of the IC with shielded enclosure in our method is equivalent to the dipole array constructed in Section 3.1. While the MOM needs to directly mesh the structures of the IC with shielded enclosure, the TL, and the ground plane.

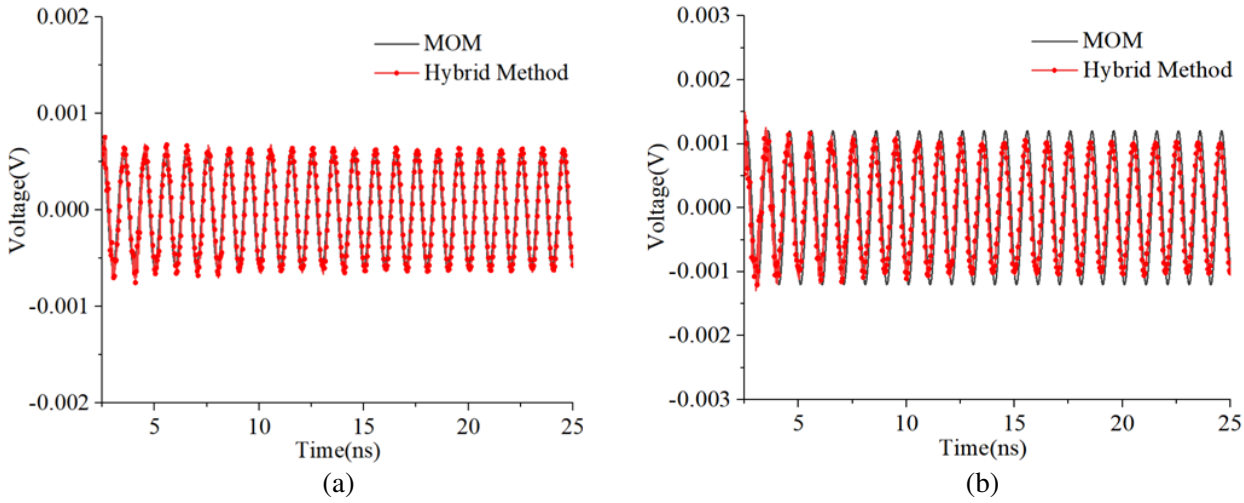

Figure 7. Voltages on the terminal loads computed by two methods for the first case: (a) voltages on R_1, (b) voltages on R_2.

It can be seen that the amplitudes and oscillation periods of the results obtained by the two methods are in good consistency. The computation time required by the proposed method and MOM is 168 s and 420 s, respectively, which means that the proposed method saves amount of computation time compared to that of full wave algorithm, because the direct mesh division of the fine structures of the IC with shielded enclosure and the TL is not needed in our method.

Figure 8 is the coupling model of the TL in the shielded enclosure excited by the leakage EM fields arising from the IC, where the dimension and thickness of the outer enclosure are $L_c \times W_c \times H_c = 60\,\text{cm} \times 60\,\text{cm} \times 60\,\text{cm}$ and 1 cm, respectively. The upper surface of the enclosure has three slots with size $L_s \times W_s = 20\,\text{cm} \times 2\,\text{cm}$, and the distance d_s from the left surface of the enclosure to the slot is 9 cm. The structure parameters and the terminal loads of the TL are the same as that of first case. The distance d of the TL to the inner enclosure is also 4 cm. To improve the efficiency of the FDTD method applied to the excitation field calculation of the TL, an auto mesh generator technique [26] is introduced to realize the fast grid division of the outer shielded enclosure in FDTD simulation. The maximum and minimum mesh sizes used by the proposed method are also 1 cm and 3 mm, respectively.

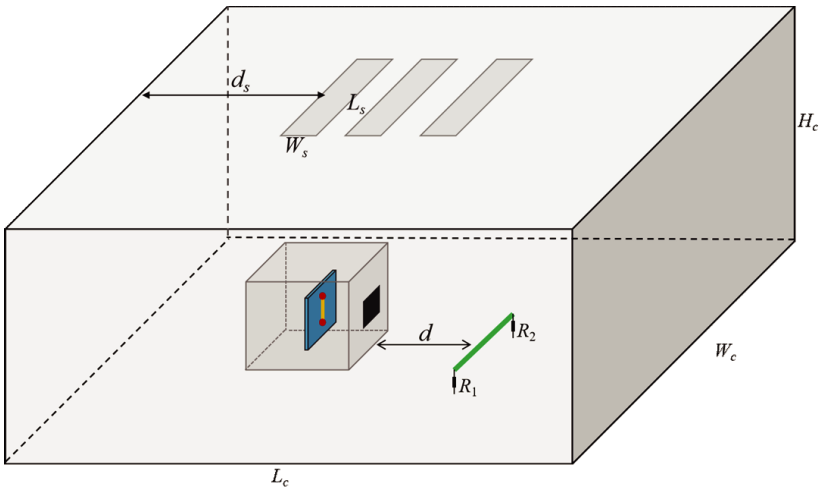

Figure 8. Coupling model of the TL excited by the leakage EM fields in shielded enclosure.

The transient voltages on the load R_1 computed by the proposed method and the MOM are shown in Fig. 9. We can see that the amplitudes and oscillation periods of the results of the two methods are also in good agreement even in the complex environment.

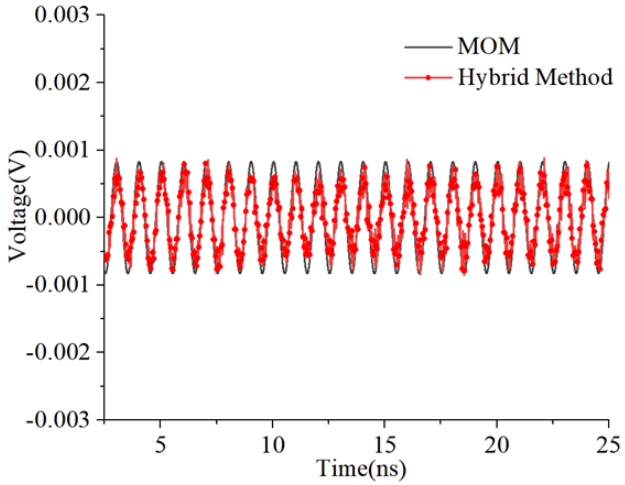

Figure 9. Voltages on the load R_1 computed by two methods for the second case.

4. CONCLUSION

To overcome the modeling difficulty of the coupling analysis of the transmission line excited by the leakage EM fields arising from the integrated circuit in shielded enclosure, an efficient time domain hybrid method consisting of a source reconstruction method based on the DDE algorithm, transmission line equations, and FDTD method with nonuniform grid technique is presented. In this method, the equivalent dipole array representing the leakage EM radiation of the IC in shielded enclosure is constructed, and the coupling model of the TL excited by the radiation fields of the dipole array is established and solved by the FDTD method with nonuniform grid technique to obtain the transient responses on the TL and its terminal loads. In summary, the significant features of this proposed method are that it can avoid modeling the fine structures of the IC with shielded enclosure and the TL directly, and realize the synchronous calculation of the leakage EM field radiation and the transient responses on the TL.

ACKNOWLEDGMENT

This work was supported by the Special Support for Chongqing Postdoctoral Research Project (Grant No. 2022CQBSHTB3018) and the Graduate Scientific Research Innovation Project of Chongqing (Grant No. CYS21297).

REFERENCES

1. Gao, Z., X. C. Li, and J. F. Mao, "Equivalent radiation source reconstruction based on artificial neural network for electromagnetic interference prediction," *Asia-Pacific International Symposium on Electromagnetic Compatibility (APEMC)*, 1–4, Nusa Dua, Bali, Indonesia, 2021.
2. Shu, Y. F., X. C. Wei, R. Yang, and E. X. Liu, "An iterative approach for EMI source reconstruction based on phaseless and single-plane near-field scanning," *IEEE Transactions on Electromagnetic Compatibility*, Vol. 60, No. 4, 937–944, 2018.
3. Liu, Q. F., N. Chao, H. Q. Zhang, and W. Y. Yin, "Lumped-network FDTD method for simulating transient responses of RF amplifiers excited by intentional electromagnetic interference signals," *IEEE Transactions on Electromagnetic Compatibility*, Vol. 63, No. 5, 1512–1521, 2021.
4. Rajamani, V., C. F. Bunting, M. D. Deshpande, and Z. A. Khan, "Validation of modal/MoM in shielding effectiveness studies of rectangular enclosures with apertures," *IEEE Transactions on Electromagnetic Compatibility*, Vol. 48, No. 2, 348–353, 2006.
5. Carpes, W. P., L. Pichon, and A. Razek, "Analysis of the coupling of an incident wave with a wire inside a cavity using an FEM in frequency and time domains," *IEEE Transactions on Electromagnetic Compatibility*, Vol. 44, No. 3, 470–475, 2002.
6. Tong, X., D. W. P. Thomas, A. Nothofer, P. Sewell, and C. Christopoulos, "Modeling electromagnetic emissions from printed circuit boards in closed environments using equivalent dipoles," *IEEE Transactions on Electromagnetic Compatibility*, Vol. 52, No. 2, 462–470, 2010.
7. Li, P., F. R. Yang, and W. Y. Xu, "An efficient approach for analyzing shielding effectiveness of enclosure with connected accessory based on equivalent dipole modeling," *IEEE Transactions on Electromagnetic Compatibility*, Vol. 58, No. 1, 103–110, 2016.
8. Ji, Z., D. Pommerenke, and J. Fan, "Determining equivalent dipoles using a hybrid source-reconstruction method for characterizing emissions from integrated circuits," *IEEE Transactions on Electromagnetic Compatibility*, Vol. 59, No. 2, 567–575, 2017.
9. Zhang, L. Y., L. Zhang, B. Wang, S. Liu, and C. Papavassiliou, "Hybrid prediction method for the electromagnetic interference characteristics of printed circuit boards based on the equivalent dipole model and the finite-difference time domain method," *IEEE Access*, Vol. 6, 6520–6529, 2018.
10. Shu, Y. F., X. C. Wei, J. Fan, R. Yang, and Y. B. Yang, "An equivalent dipole model hybrid with artificial neural network for electromagnetic interference prediction," *IEEE Transactions on Microwave Theory and Techniques*, Vol. 67, No. 5, 1790–1797, 2019.

11. Wen, J., L. Ding, Y. L. Zhang, and X. C. Wei, "Equivalent electromagnetic hybrid dipole based on cascade-forward neural network to predict near-field magnitude of complex environmental radiation," *IEEE Journal on Multiscale and Multiphysics Computational Techniques*, Vol. 5, 227–234, 2020.
12. Wen, J., X. C. Wei, Y. L. Zhang, and T. H. Song, "Near-field prediction in complex environment based on phaseless scanned fields and machine learning," *IEEE Transactions on Electromagnetic Compatibility*, Vol. 63, No. 2, 571–579, 2021.
13. Xiang, F. P., E. P. Li, X. C. Wei, and J. M. Jin, "A particle swarm optimization-based approach for predicting maximum radiated emission from PCBs with dominant radiators," *IEEE Transactions on Electromagnetic Compatibility*, Vol. 57, No. 5, 1197–1205, 2015.
14. Wang, B. F., E. N. Liu, W. J. Zhao, and C. E. Png, "Reconstruction of equivalent emission sources for PCBs from near-field scanning using a differential evolution algorithm," *IEEE Transactions on Electromagnetic Compatibility*, Vol. 60, No. 6, 1670–1677, 2018.
15. Song, T. H., X. C. Wei, J. J. Ju, W. T. Liang, and R. X. K. Gao, "An effective EMI source reconstruction method based on phaseless near-field and dynamic differential evolution," *IEEE Transactions on Electromagnetic Compatibility*, Vol. 64, No. 5, 1506–1513, 2022.
16. Xie, L. and Y. Z. Lei, "Transient response of a multiconductor transmission line with nonlinear terminations excited by an electric dipole," *IEEE Transactions on Electromagnetic Compatibility*, Vol. 51, No. 3, 805–810, 2009.
17. Yan, L. P., X. D. Zhang, X. Zhao, and X. L. Zhou, "A fast and efficient analytical modeling approach for external electromagnetic field coupling to transmission lines in a metallic enclosure," *IEEE Access*, Vol. 6, 50272–50277, 2018.
18. Wang, X. J., L. X. Wang, J. L. Zhou, X. Lu, M. J. Yuan, and J. Y. Zhou, "A hybrid CN-FDTD-SPICE solver for field-circuit analyses in low-frequency wideband problems," *IEEE Transactions on Components, Packaging and Manufacturing Technology*, Vol. 10, No. 10, 1721–1728, 2020.
19. Seifi, Z., A. Ghorbani, and A. Abdipour, "Time-domain analysis and experimental investigation of electromagnetic wave coupling to RF/microwave nonlinear circuits," *Journal of Electromagnetic Waves and Applications*, Vol. 35, No. 1, 51–70, 2021.
20. Ye, Z. H., C. C. Lu, and Y. Zhang, "Coupling analysis of penetrated wire connecting two electronic devices using a time domain hybrid method," *Microwave and Optical Technology Letters*, Vol. 63, No. 9, 2359–2363, 2021.
21. Yan, Y. J., L. Meng, X. L. Liu, T. Y. Jiang, J. Chen, and G. J. Zhang, "An FDTD method for the transient terminal response of twisted-wire pairs illuminated by an external electromagnetic field," *IEEE Transactions on Electromagnetic Compatibility*, Vol. 60, No. 2, 435–443, 2018.
22. Ye, Z., X.-Z. Xiong, C. Liao, and Y. Li, "A hybrid method for electromagnetic coupling problems of transmission lines in cavity based on FDTD method and transmission line equation," *Progress In Electromagnetics Research M*, Vol. 42, 85–93, 2015.
23. Slattery, K. and C. Wei, "Measuring the electric and magnetic near fields in VLSI devices," *IEEE International Symposium on Electromagnetic Compatibility*, Vol. 2, 887–892, Seattle, WA, USA, 1999.
24. Qing, A., "Dynamic differential evolution strategy and applications in electromagnetic inverse scattering problems," *IEEE Transactions on Geoscience and Remote Sensing*, Vol. 44, No. 1, 116–125, 2006.
25. Rotgerink, J. L., R. Serra, and F. Leferink, "Multiconductor transmission line modeling of crosstalk between cables in the presence of composite ground planes," *IEEE Transactions on Electromagnetic Compatibility*, Vol. 63, No. 4, 1231–1239, 2021.
26. MacGillivray, J. T., "Trillion cell CAD-based cartesian mesh generator for the finite-difference time-domain method on a single-processor 4-GB workstation," *IEEE Transactions on Antennas and Propagation*, Vol. 56, No. 8, 2187–2190, 2008.